Nanoscience and
Nanotechnology Letters
Vol. 7, 1–5, 2015

Surface Periodic Nanostructure of *p*-GaSb Irradiated by Femtosecond Laser and Optical Properties Research

Xian Gao[1], Jilong Tang[1,*], Dan Fang[1], Shuangpeng Wang[2], Xiaohui Ma[1], Haifeng Zhao[2], Xuan Fang[1], Yongfeng Li[3], Xiaohua Wang[1], Zhikun Xu[4], and Zhipeng Wei[1]

[1]*State Key Laboratory on High-Power Semiconductor Lasers, School of Science, Changchun University of Science and Technology, Changchun 130022, China*
[2]*Key Laboratory of Excited State Process, Changchun Institute of Optics, Fine Mechanics and Physics, Chinese Academy of Science, Changchun 130033, China*
[3]*Key Laboratory of Physics and Technology for Advanced Batteries, Ministry of Education, College of Physics, Jilin University, Changchun 130012, China*
[4]*Harbin Normal University, Harbin 150080, China*

We report the fabrication of nanostructures on *p*-GaSb surface using femtosecond laser. The scanning electron microscopy images suggest that the nanoscale ripples appeared with the condition of femtosecond laser-induced pulse energy between 30 mJ/cm^2 and 90 mJ/cm^2, and the surface ripples orientation perpendicular to the polarization direction of the incident laser. Period of the nanostructures are 460–770 nm, shorter than the laser wavelength and appears as a result of surface instability. In addition, for further research on optical properties, the nanostructures were characterized by low-temperature photoluminescence spectra, Raman spectra and X-ray diffraction. All the results indicate that the different defects and nanostructures are formed in the surface of the laser-induced samples.

Keywords: Femtosecond Laser, GaSb Periodic Nanostructures, Photoluminescence, Raman Spectrum, X-ray Diffraction.

1. INTRODUCTION

GaSb is an important III–V compound semiconductor material due to its low band gap of 0.7 eV and the high mobility of hole. Unintentionally doped GaSb wafers are always *p*-type conductive properties because of native lattice defects. GaSb-based semiconductor alloys have great potential applications in mid-infrared optoelectronics and thermophotovoltaics.[1–4] However, the achievement of these materials have been blocked by their uncontrolled surface properties. Various chemical and phyical treatments of GaSb with the aim to improve and develop the surface properties for further applications.[5] Low-dimensional nanostructures, such as quantum dots and quantum wires, are of particular interest since they exhibit better optoelectronic properties and superior device performance, such as narrower spectra linewidth, lower threshold current density, and reduced temperature sensitivity, as compared to thin films. Thus nanostructure materials have potential applications in many fields, such as physicochemical field, biomedical field, manufacture grating and batteries.[6–10]

Femtosecond laser is uaually utilized to induce periodic nano-/micro-structures since this phenomenon are observed by Birnbaum.[11] Many research focus on this phenomenon and periodic nano-/micro-structures have been fabricated on many materials successfully, such as metals,[12,13] semiconductors[14–19] and dielectrics.[20,21] The formation of such periodic two-dimensional structures was attributed to optical interference of the incident laser light with scattered waves from a surface disturbance.[2,5] Recently, the energy density threshold value of the femtosecond laser could be controlled precisely with the development of technology, thus femtosecond laser technique becomes an important tool for micro-process of submicron range, and has great potential to manufacture grating, optical waveguides, batteries and other micro- and optoelectronic devices.[9] Femtosecond laser irradiation on semiconductors has led to nano-/micro-structures of different sizes and shapes and the theoretical modeling on silicon was established.[22,23]

In this paper, the periodic nanostructure on *p*-GaSb surface was manufactured using femtosecond laser, and the optical properties of the ablation surface were investigated

*Author to whom correspondence should be addressed.

 1941-4900/2015/7/001/005 doi:10.1166/nnl.2015.1926

in detail. The surface was examined with the use of scanning electron microscopy (SEM) to analyze morphology of the surface and photoluminescence (PL) spectra, Raman spectra and X-ray Diffraction (XRD) to analyze its optical properties, chemical composition and structure properties.

2. EXPERIMENTAL DETAILS

The single side polished (100) oriented undoped GaSb wafer with the thickness of 500 μm was used in the experiments. The samples were irradiated in vacuum using linearly polarised femtosecond laser.

The laser-induced system consists of an amplified Ti:sapphire femtosecond laser system with the central wavelength is 800 nm, frequency is 1 kHz and pulse duration is 50 fs. In addition, scanning speed and scanning spacing are 3 mm/s and 50 μm, respectivly. The pulse energy is limited to 30 mJ/cm^2, 60 mJ/cm^2 and 90 mJ/cm^2 using neutral density filters on purpose, and laser polarization direction is parallels to the scanning direction with the incident angle of 90°.

The surface morphologies of the samples were characterized via scanning electron microscope (SEM, JEOL-6010LA). PL9000 Fourier transform spectrometer was used to study the low temperature photoluminescence (PL) spectrum. In the measurement process, an Ar ion laser with 514 nm line and liquid nitrogen was applied to Ge cooled detector, and the laser power was set to 40 mW. Raman spectroscopy was used to obtain information concerning about the crystalline structure of the ablated area, and the surfaces were excited by Ar ion laser with the 532 nm emission line. Raman spectra were recorded in 180° backscatter geometry on samples oriented perpendicularly to the excitation beam direction (z) with liquid nitrogen cooled CCD-multichannel detector. X-ray Diffraction (Bruker AXS D8 DAVINCI) with Cu-Ka radiation ($\lambda = 1.5406$ Å) were utilize to further research on optical properties of the p-GaSb samples.

3. RESULTS AND DISCUSSION

Figures 1(a), (c) and (e) show the SEM images of the surface morphology of p-GaSb after treatment via

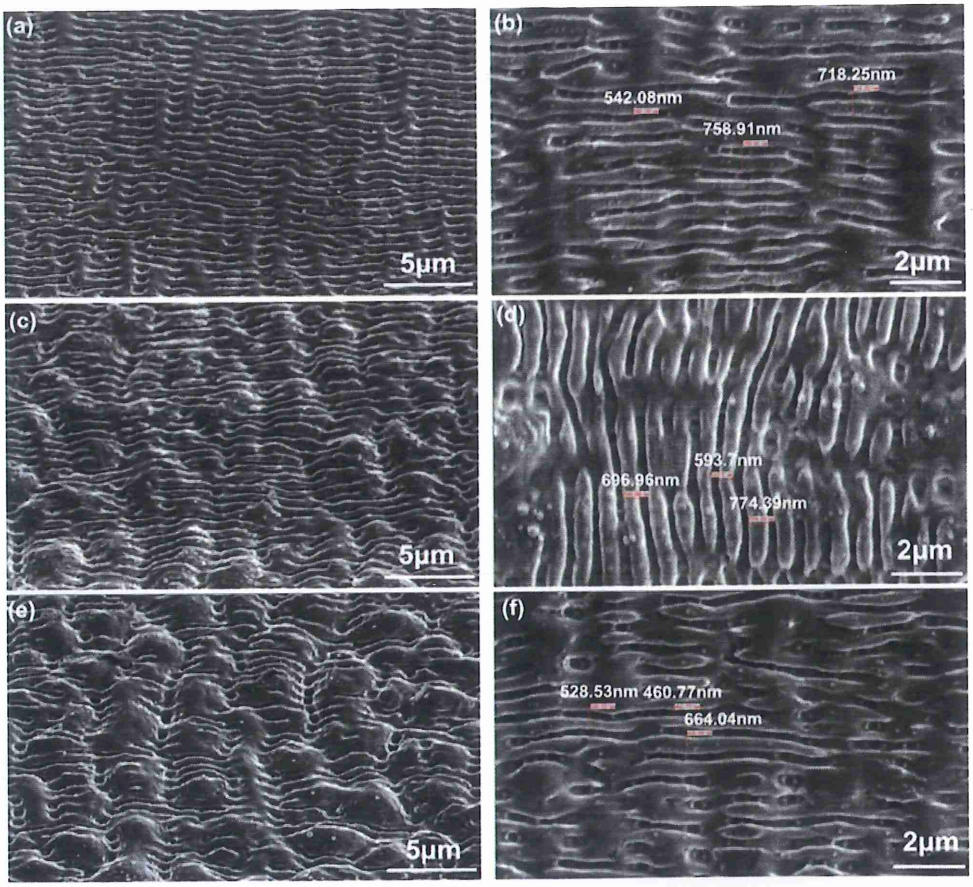

Fig. 1. SEM image of the surface topography of p-GaSb after treatment of femtosecond laser. (a) pulse energy of 30 mJ/cm^2 and amplification is 5000 with slant angle of 45°, (b) pulse energy of 30 mJ/cm^2 and amplification is 10000 with slant angle of 90°, (c) pulse energy of 60 mJ/cm^2 and amplification is 5000 with slant angle of 45°, (d) pulse energy of 60 mJ/cm^2 and amplification is 10000 with slant angle of 90°, (e) pulse energy of 90 mJ/cm^2 and amplification is 5000 with slant angle of 45°, (f) pulse energy of 90 mJ/cm^2 and amplification is 10000 with slant angle of 90°.

femtosecond laser with pulse energy of 30 mJ/cm^2, 60 mJ/cm^2 and 90 mJ/cm^2 and with the slant angle of 45°. It can be observed clearly that the periodic nanostructures were fabricated on the surface. The laser-induced surface ripples orientation favors the direction perpendicular to the polarization of the incident laser radiation, and this result in agreement with previous reports on other semiconductor materials like InP and silica.[17, 24–27] We found the ripples of *p*-GaSb appeared when appropriate pulse energy was used. The nanostructure formed when the pulse energy was closed to 30 mJ/cm^2, and became clear and periodicity when the pulse energy is 60 mJ/cm^2. These periodic nanostructures became indistinct with the pulse energy increasing. The ripples were melt down when the pulse energy reaching 90 mJ/cm^2, and with the energy increased continuously the groove between the ripples disappeared gradually as shown in Figure 1(e).

Figures 1(b), (d), (f) show the surface morphology fabricated by femtosecond laser with pulse energy of 30, 60 and 90 mJ/cm^2 with slant angle of 90°. The width of the ripples is in the range of 460 nm to 774 nm. In addition, with the laser-induced pulse energy are increasing, the period only trend to decrease with the increase of the laser pulse energy. In the group of J. Bonse's researches, the spatial periods of the ripples coincide with the laser radiation wavelength, while their orientation favors the direction perpendicular to the polarization of the incident laser radiation.[17]

Figure 2(a) shows the low temperature photoluminescence (PL) spectra of the *p*-GaSb samples which were laser treated with pulse energy of 60 mJ/cm^2 and untreated *p*-GaSb sample at 20 K. The PL spectrum of untreated GaSb shows the donor–acceptor (D–A) pair transition at 773 meV (marked 1) and acceptor bound exciton of $V_{Ga}Ga_{Sb}$ at 792 meV (marked 2),[28, 29] whereas for laser-treated GaSb, the main peaks at 752 meV (marked 3) with a shoulder at 758 meV (marked 4) can be attributed to a triple native defect $V_{Ga}Ga_{Sb}V_{Ga}$.[30, 31] Proved more different defects are formed after laser treatment. The other peaks at 796 meV (marked 5) and 817 meV (marked 6) are observed, the former can be ascribed to acceptor bound exciton of $V_{Ga}Ga_{Sb}$, and the latter is related to the band gap. Dutta suggested that the broad peak (marked 7) is attributed to the thick native oxide layer present on the sample surface.[32] Another research on InP nanostructures PL point out this broad PL band associated with a large size distribution of InP surface.[33] Figure 2(b) shows the normalized temperature-dependent PL spectra of the *p*-GaSb samples. It can be observed that the peaks marked 1, 2, 3, 4 and 6 (817 meV) are slightly red-shift with the increasing of temperature, originating from the band gap of the bulk GaSb decreases primarily due to electron-phonon interaction and partially due to thermal expansion. The peak locates at 796 meV (marked 5) decay with the increasing temperature. However, the broad peak between

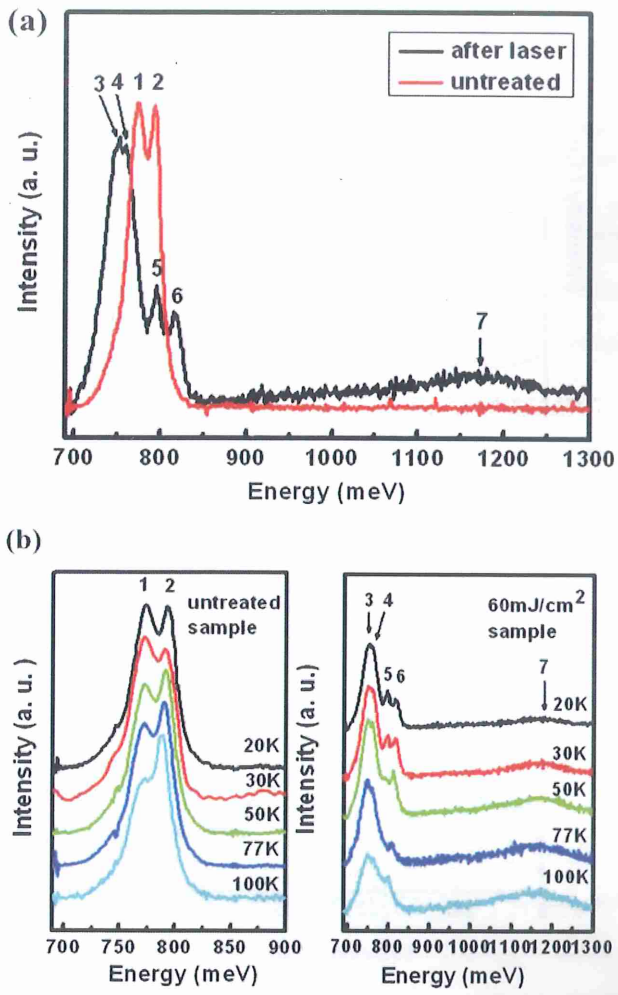

Fig. 2. (a) Low temperature photoluminescence spectra of *p*-GaSb that untreated sample and 60 mJ/cm^2 laser treated sample at 20 K. (b) The normalized temperature-dependent spectra of the *p*-GaSb samples, the untreated sample on the left and the 60 mJ/cm^2 treated sample on the right.

1.0 eV to 1.3 eV has a trend to increase with the increasing temperature. We speculate the broad PL band is ascribed to complex interaction of the nanostructures and the surface oxides. Defects related peaks decayed with the increase of the temperature, and the nanostructures related peaks are gradually increased.

Figure 3(a) shows room temperature Raman spectra of the samples. The black curve belongs to untreated *p*-GaSb sample, and the longitudinal optical (LO) phonon-peak appeared at about 238 cm^{-1} can be corresponding to the typical Raman spectrum for GaSb.[34] The appearance of this line was consistent with the selection rules for the GaSb (100) orientation[35] and the weak second order combinational scattering features appears in 267 cm^{-1} [36–38] could also be detected. The other three curves belong to laser-induced samples and treated with laser pulse power of 30 mJ/cm^2, 60 mJ/cm^2 and 90 mJ/cm^2, respectively. Apparently, the line locates at 225 cm^{-1} can be attributed

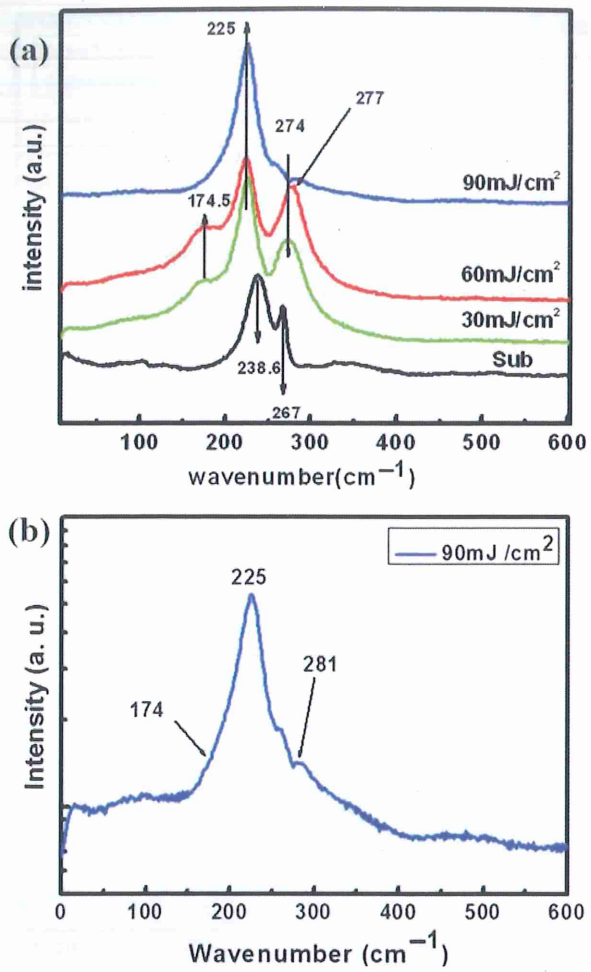

Fig. 3. (a) Room-temperature Raman spectra on *p*-GaSb surface. (b) Raman spectra of GaSb sample with laser-induced pulse energy of 90 mJ/cm^2.

to the LO phonon peak. Compared with untreated sample, the line at 238.6 cm^{-1} shift to longer wavelengths indicated that there was a nanocrystalline phase,[39] this phenomenon corresponding to the nanostructures formed in the surface in the laser-induced sample as the SEM image shown. Besides, transverse optical (TO) phonon-peak appeared at 30 mJ and 60 mJ curves in 174 cm^{-1} related to the change of the lattice plane, indicated that the nanostructures appeared on the surface. The peaks locate at 274 cm^{-1}, 277 cm^{-1} (Fig. 3(a)) and 281 cm^{-1} (Fig. 3(b)) were ascribed to the shift of the weak second order combinational scattering features. The peaks at 174 cm^{-1} and 281 cm^{-1} became very weak in the condition of laser pulse energy is 90 mJ/cm^2 as shown in Figure 3(b). We assume these decrease are a kind of response of the destruction of the lattice perfection which are caused by the overdose laser pulse energy.

Figure 4 shows the XRD patterns measured from GaSb samples, (a) GaSb substrate, and the others are laser-induced sample: laser pulse energy of (b) 30 mJ/cm^2, (c) 60 mJ/cm^2, (d) 90 mJ/cm^2. The main two peaks locate

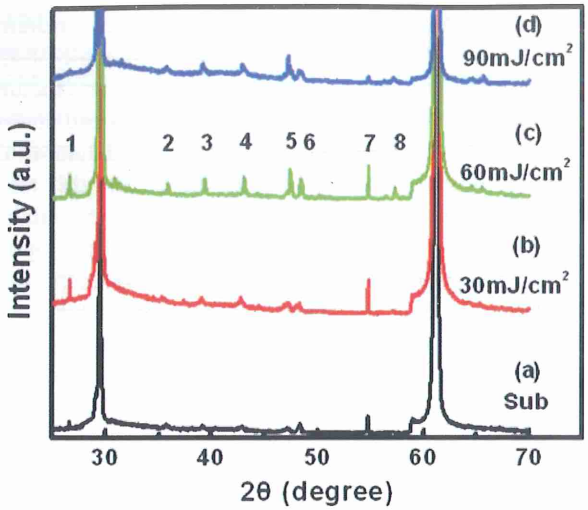

Fig. 4. The XRD 2θ scan curves measured from GaSb samples, (a) GaSb substrate, laser-induced sample: laser pulse energy of (b) 30 mJ/cm^2, (c) 60 mJ/cm^2, (d) 90 mJ/cm^2.

at 29.5° and 61.2° suggest that the substrate is GaSb. There are many other peaks exist in the curves. The peaks located at 26.6°, 35.8°, 23.2°, 47.3°, 48.4°, 54.7° and 57.3° in the figure are marked from 1 to 8, respectively. These peaks belong to Gallium Oxide and Antimony Oxide. It is sure that these small sharp peaks have the strongest values when the laser-induced pulse energy is 60 mJ/cm^2. This phenomenon is pointed out laser-induced process could produce Gallium Oxide and Antimony Oxide. However, these peaks become weak when the pulse energy is 90 mJ/cm^2, even lower than the substrate sample. The basic assumptions as followed. We assume the laser-induced process destroy the bond between Ga and Sb at lower pulse energy, and dangling bond formed in the surface of the GaSb. More defects formed in the sample surface, later Ga oxides and Sb oxides are formed in the air. But a large number of Ga and Sb atoms are divided from the surface when laser pulse energy reached 90 mJ/cm^2, oxides are not formed easily as lower laser-induced pulse energy. Finally, the lattice perfection is destroyed. This hypothesis is also fit the PL and Raman results.

4. CONCLUSIONS

In conclusion, we fabricate periodic nanostructures on *p*-GaSb by femtosecond laser. The optimal value of the pulse energy of laser to make the periodic nanostructure shown on *p*-GaSb is between 30 mJ/cm^2 and 90 mJ/cm^2. The properties were investigated by SEM images, XRD, low temperature PL spectra and Raman spectra. The laser-induced surface ripples were perpendicular to the laser polarization direction, and the ripples period are between 460 nm to 770 nm. The low temperature PL spectra suggest that more defects formed in the surface and the nanostructures related peak shown after laser-induced. Laser

induced structure can affect Raman peak position and make the Full Wave at Half Maximum (FWHM) broad. The XRD results point out the process of Ga oxides and Sb oxides formed. These phenomena corresponding to the different defects and nanostructures are formed in the surface of the laser-induced samples.

Acknowledgment: This work is supported by the National Natural Science Foundation of China (61076039, 61204065, 61205193, 61307045), Research Fund for the Doctoral Program of Higher Education of China (20112216120005), the Developing Project of Science and Technology of Jilin Province (20121816, 201201116), National Key Lab of High Power Semiconductor Lasers Foundation (No. 9140C310101120C031115).

References and Notes

1. S. C. Chen and Y. K. Su, *J. Appl. Phys.* 66, 350 (**1989**).
2. L. Reijnen, R. Brunton, and I. R, *AIP Conf. Proc.* 738, 360 (**2004**).
3. M. G. Mauk, Z. A. Shellenbarger, J. A. Cox, O. V. Sulima, A. W. Bett, R. L. Mueller, P. E. Sims, J. B. McNeely, and L. C. DiNetta, *J. Cryst. Growth.* 211, 189 (**2000**).
4. A. W. Bett and O. V. Sulima, *Semicond. Sci. Technol.* 18, 184 (**2003**).
5. E. Papis-Polakowska, *Electron Technology: Internet Journal* 37/38, (**2005/2006**).
6. W. Xuan, C. Zhu, Y. Liu, and Y. Cui, *Soc. Rev.* 41, 1677 (**2012**).
7. K. Ariga, Q. Ji, J. P. Hill, Y. Bando, and M. Aono, *NPG Asia Mater.* 4, 17 (**2012**).
8. H. Sunhwan, L. Joongwon, H. U. Gi, J. J. Chul, B. J. Hyun, K. D. Jun, L. Hyojun, and S. I. Kyu, *J. Nanosci. Nanotechnol.* 12, 6051 (**2012**).
9. N. Agnes, H. Y. Tao, Z. Q. Hao, C. K. Sun, X. Gao, and J. Q. Lin, *Chin. Phys. B* 22, 014209 (**2013**).
10. C. Wang, G. C. Lim, and F. L. Ng, *Surf. Rev. Lett.* 12, 651 (**2005**).
11. M. Birnbaum, *J. Appl. Phys.* 36, 657 (**1965**).
12. A. Y. Vorobyev and C. L. Guo, *Phys. Rev. B* 72, 195422 (**2005**).
13. A. Chimmalgi, T. Y. Choi, C. P. Grigoropoulos, and F. K. Komvopoulos, *J. Appl. Phys.* 97, 104319 (**2005**).
14. A. Borowiec, M. Couillard, G. A. Botton, and H. K. Haugen, *Appl. Phys. A* 79, 1887 (**2004**).
15. A. Borowiec, M. Mackenzie, G. C. Weatherly, and H. K. Haugen, *Appl. Phys. A* 77, 201 (**2003**).
16. J. Bonse, S. M. Wiggins, and J. Solis, *Appl. Surf. Sci.* 248, 243 (**2005**).
17. J. Bonse, J. M. Wrobel, J. Kruger, and W. Kautek, *Appl. Phys. A* 72, 89 (**2001**).
18. J. Bonse, M. Munz, and H. Sturm, *J. Appl. Phys.* 97, 013538 (**2005**).
19. J. Bonse, J. M. Wrobel, K. W. Brzezinka, N. Esser, and W. Kautek, *Appl. Surf. Sci.* 202, 272 (**2002**).
20. T. Q. Jia, H. X. Chen, M. Hung, F. L. Zhao, J. R. Qiu, R. X. Li, Z. Z. Xu, X. K. He, J. Zhang, and H. Kuroda, *Phys. Rev. B* 72, 125429 (**2005**).
21. N. Yasumaru, K. Miyazki, and J. Kiuchi, *Appl. Phys. A* 81, 933 (**2005**).
22. Anil Kumar Singh and R. K. Soni, *AIP Conference Proceedings* 1147, 172 (**2009**).
23. H. Y. Tao, J. Q. Lin, Z. Q. Hao, X. Gao, X. W. Song, C. K. Sun, and X. Tan, *J. Appl. Phys.* 100, 201111 (**2012**).
24. H. X. Qian and W. Zhou, *International Journal of Nanoscience* 4, 779 (**2005**).
25. S. Hohm, A. Rosenfeld, J. Kruger, and J. Bonse, *J. Appl. Phys.* 112, 014901 (**2012**).
26. M. Rohloff, S. K. Das, S. Hohm, R. Grunwald, A. Rosenfeld, J. Kruger, and J. Bonse, *J. Appl. Phys.* 110, 014910 (**2011**).
27. F. Costache, S. Kouteva-Arguirova, and J. Reif, *Appl. Phys. A* 79, 1429 (**2004**).
28. P. S. Dutta, K. S. Sangunni, and H. L. Bhat, *Appl. Phys. Lett.* 65, 1695 (**1994**).
29. P. S. Dutta, A. K. Sreedhar, and H. L. Bhat, *J. Appl. Phys.* 79, 3246 (**1996**).
30. P. S. Dutta, V. Prasad, and H. L. Bhat, *J. Appl. Phys.* 80, 2847 (**1996**).
31. P. S. Dutta and H. L. Bhat, *J. Appl. Phys.* 81, 5821 (**1997**).
32. P. S. Dutta, K. S. R. Koteswara Rao, and H. L. Bhat, *J. Appl. Phys.* 77, 4825 (**1995**).
33. S. S. Tian, Z. P. Wei, H. F. Zhao, X. Gao, X. Fang, J. L. Tang, and X. H. Ma, *Nanosci. Nanotechnol. Lett.* 5, 1274 (**2013**).
34. P. S. Dutta, K. S. R. Koteswara Rao, H. L. Bhat, and V. Kumar, *Appl. Phys. A* 61, 149 (**1995**).
35. L. Reijnen, R. Brunton, and I. R. Grant, *AIP Conference Proceedings* 738, 360 (**2004**).
36. S. G. Kim, H. Asahi, M. Seta, and J. Takizawa, *J. Appl. Phys.* 74, 579 (**1993**).
37. Yu, A. Danilov, A. A. Biryukov, J. L. Gonçalves, J. W. Swart, F. Iikawa, and O. Teschke, *Semiconductors* 39, 132 (**2005**).
38. J. E. Maslara and W. S. Hurst, *J. Appl. Phys.* 103, 013502 (**2008**).
39. Yu, A. Danilov, A. A. Biryukov, J. L. Gonçalves, J. W. Swart, F. Iikawa, and O. Teschke, *Semiconductors* 39, 132 (**2005**).

Received: 25 May 2014. Accepted: 3 September 2014.